Repeated loss of floral scent in independent transitions from bee to hummingbird pollination in spiral gingers

Kathy Darragh[1,2,+], Kathleen M. Kay[3], Santiago R. Ramírez[1]

[1]Department of Evolution and Ecology, University of California, Davis, CA, USA

[2]Department of Biology, Indiana University, Bloomington, IN, USA

[3]Department of Ecology and Evolutionary Biology, University of California, Santa Cruz, CA, USA

[+]Corresponding author (Email: kdarrag@iu.edu)

ORCID Kathy Darragh 0000-0002-9215-014X

ORCID Kathleen M. Kay 0000-0001-8858-110X

ORCID Santiago R. Ramírez 0000-0003-1306-1315

Keywords

Convergent evolution, floral scent, hummingbird, orchid bee, pollination, spiral gingers, transcriptomics, trait evolution

Abstract

The repeated evolution of the same trait in different lineages provides powerful natural experiments to study the phenotypic and genotypic predictability of how traits are gained and lost. A fascinating example of this is the repeated evolution of hummingbird pollination in plant lineages in the Americas, a widespread and seemingly unidirectional phenomenon. The spiral gingers in the genus *Costus* are ancestrally bee-pollinated and hummingbird pollination has evolved multiple times independently in the tropical Americas. These pollinator transitions are accompanied by predictable morphological and color changes but the changes in floral scent have not been described. In this study, we describe the floral scent composition of 29 species of *Costus* sampled across the phylogeny to understand how floral scent has evolved across the genus with respect to pollinator transitions. We then combine transcriptomics and genomics in one clade of *Costus* to identify genetic expression differences and gene family evolution associated with pollinator transitions. We show that hummingbird-pollinated species have mostly lost their floral scent, whereas bee-pollinated species exhibit either floral scent maintenance or in some cases, gains of more diverse scent profiles. The remarkable consistency of scent loss in hummingbird-pollinated species highlights the shared strong selection pressures experienced by these lineages. Even species with more recent transitions from bee to hummingbird pollination exhibit scent loss, highlighting the rapid breakdown of scent production following pollinator transitions. We also find the floral scent loss appears to be due to gene downregulation rather than pseudogenization. This research highlights the capacity for rapid changes when selection pressures are strong through downregulation of floral scent genes.

Introduction

The repeated evolution of the same traits in different lineages is thought to reflect shared selection pressures. These cases of repeated evolution apply not only to the gain of traits, such as the evolution of antifreeze proteins in fish (Chen et al. 1997) or carnivory in plants (Albert et al. 1992), but also the loss of traits, as seen in the eye regression of cavefish (Sifuentes-Romero et al. 2023), or reduction of attractive traits such as flower size or floral scent in self-fertilizing plants (Tsuchimatsu and Fujii 2022). Repeated evolution provides us with systems where we can study the process of adaptation and ask questions about the predictability of the evolution, and the extent of constraint, or flexibility, of the underlying molecular mechanisms (Orr 2005; Losos 2011; Sackton and Clark 2019).

A fascinating example of repeated evolution is pollinator transitions in flowering plants. For example, the evolution of hummingbird pollination has occurred many times across flowering plants, and often involves convergence in a suite of traits. Flowers pollinated by hummingbirds are characterized by traits thought to attract and fit hummingbirds (such as a narrow shape and large amounts of nectar) and in addition, traits thought to deter bees (red coloration, lack of nectar guides, lack of scent) (Schemske and Bradshaw 1999; Castellanos et al. 2004; Bergamo et al. 2016). Interestingly, the evolution of hummingbird pollination has only been documented in one direction, from ancestral bee pollination to derived hummingbird pollination, with the reasons for this remaining unclear (Rosas-Guerrero et al. 2014; Abrahamczyk and Renner 2015; Kay and Grossenbacher 2022).

Hummingbird-pollinated flowers are described to lack scent (Knudsen et al. 2004; Wessinger 2024), likely due to the expectation of poor smell in birds (Bang and Cobb 1968). More recent studies have found evidence for the importance of olfactory cues in birds (Hagelin 2007; Gwinner and Berger 2008; Nevitt et al. 2008). However, genomic studies have shown that, even for birds, hummingbirds have a low number of olfactory receptors (Driver and Balakrishnan 2021; Driver 2022), suggesting at least a reduced investment in this sensory modality. Behavioral experiments have also suggested that hummingbirds rely more on visual than olfactory cues when foraging (Goldsmith and Goldsmith 1982). In fact, floral scent analyses of hummingbird pollinated flowers have shown either complete lack of floral scent or low

emission rates of floral scent compounds. (Knudsen et al. 2004; Byers et al. 2014; Amrad et al. 2016).

A fascinating group in which to study the evolution of hummingbird pollination is the genus *Costus* (Costaceae). The genus contains over 80 species of perennial understory herbaceous monocots, the majority of which have diverged rapidly within the last 3 million years in Central and South America (Maas 1972, 1977; Vargas et al. 2020). Since establishing and radiating in the American tropics approximately three million years ago, hummingbird pollination has evolved repeatedly and independently in *Costus* from an ancestral state of bee pollination (Vargas et al. 2020). Specifically, bee-pollinated species are pollinated primarily by orchid bees (Apidae: Euglossini), that visit the flowers for nectar and pollen, and hummingbird-pollinated species are often pollinated by hermit hummingbirds (Kay and Schemske 2003). While different species were initially classified as hummingbird or bee pollinated (Maas 1972, 1977), many species do not fit the classic paradigms. For example, many bee-pollinated flowers have red coloration (Kay and Schemske 2003), and hummingbird-pollinated flowers are short (Yost and Kay 2009). Despite this variation, a single phenotypic optimum is shared across most of the independent transitions to hummingbird pollination in the clade (Kay and Grossenbacher 2022). Traits including small flower size, the absence of nectar guides, and brightly colored floral bracts are all predictive of hummingbird pollination (Kay and Grossenbacher 2022). The combination of recent genomic resources, a well-resolved phylogeny, and the possibility of collecting samples both in the field and in greenhouses, makes *Costus* a powerful system to study the evolution of convergence on hummingbird pollination (Vargas et al. 2020; Kay and Grossenbacher 2022; Harenčár et al. 2023).

While the morphological and color changes involved in the evolution of hummingbird pollination have been well-studied in *Costus*, the expected scent changes have not been characterized. In this study, we describe floral scent in 29 species of *Costus* sampled across the phylogeny. We test for differences in floral scent between bee-pollinated and hummingbird-pollinated species and investigate how floral scent has evolved across the genus. We then focus on one clade of *Costus* with variation in floral scent production and generate floral transcriptomic data. We use this data to identify gene expression differences associated with floral scent production, helping us to better understand the genetic changes underlying floral scent evolution in this group. Finally, we annotated the terpene synthase genes (TPS) in three

previously available *Costus* genomes, and a high-quality genome assembly for *Costus allenii* generated in this study. High-quality annotations allow us to analyze the evolution of this gene family that plays an important role in floral scent evolution. Our study, therefore, combines multiple approaches to characterize floral scent changes, gene expression changes, and gene family evolution associated with shifts to hummingbird pollination in *Costus*.

Materials and Methods

Floral scent sample collection

We collected 101 samples of 29 species of *Costus* between 2019 and 2023 (Table S1). All samples for *Costus glaucus*, *Costus laevis*, *Costus montanus*, *Costus stenophyllus*, and *Costus wilsonii* were collected in Costa Rica (La Gamba, Las Cruces, Las Alturas, and Monteverde). All other species were sampled in the UCSC greenhouses in Santa Cruz, California, USA from plants composing the UCSC living *Costus* collection. For each day of sampling, both floral scent samples and ambient samples were collected (with one exception: a *Costus scaber* sample collected on April 8th 2019 was missing a control and so we used a control from the nearest date available, March 7th). Scent was sampled using dynamic headspace sampling. Flowers from living plants were placed inside oven bags (Reynold's). A Spectrex PAS-500 air pump with taigon tubing was used to pull scented-air through a volatile trap for 6 hours at a flow rate of 200 ml air / min. The volatile trap contained a filter of glass wool and 50 mg Porapak. We conditioned scent traps by passing 5 mL of hexane before usage. Volatiles were eluted from the trap using 400µl of hexane and stored at -20°C.

Chemical analysis

Samples were analyzed using Agilent model 5977A mass-selective detector with an Agilent GC model 7890B. Samples were run on a HP-5 Ultra Inert column (Agilent, 30m x 0.25mm, 0.25 µm). For analysis, one microliter of each sample was injected in splitless mode using the ALS 7694 autosampler with helium as the carrier gas (250°C injector temperature). The program started at 40 °C for 3 minutes and then rose at 5 °C/min to 210°C. The temperature was held at 210°C for 1 minute, then 300°C for 2.5 minutes, and 315°C for a final minute.

Compounds were identified by comparing mass spectra and retention indices with reference libraries. Compounds that were not found in at least two samples were removed. A

two-step process was used to filter datasets for floral scent components. First, compounds were filtered to include only those which are found in five times higher amounts in floral than ambient samples using the "filter_ambient_ratio" function from the *bouquet* package (Powers et al. 2023). This resulted in a list of ambient compounds which were not considered floral scent compounds. Second, using the raw data matrices, we subtracted the ambient compound amounts from the corresponding floral scent amount collected on the same date. We then removed the ambient compounds identified by the package *bouquet* from this subtracted matrix to create the final data matrix of floral scent.

Statistical analyses of floral scent

To visualize divergence in floral scent among samples we used nonmetric multidimensional scaling (NMDS) using the "metaMDS" function in *vegan* (Oksanen et al. 2020). To test for differences both between pollination groups, and between floral and ambient samples, we carried out a PERMANOVA (permutational multivariate analysis of variance) using the "adonis2" function in *vegan* (Bray–Curtis distance matrix, 1000 permutations). To identify which groups were significantly different, we carried out post hoc pairwise testing using the "pairwise.perm.MANOVA" function in the *RVAideMemoire* package with a Bonferroni correction (Hervé 2021). We did this for both filtered and unfiltered datasets.

We tested for differences in compound number produced by bee-pollinated and hummingbird-pollinated species using ANOVA with a nested model including species within pollinator group. To test for differences in the diversity of compounds produced by bee-pollinated and hummingbird-pollinated species, we used the package *chemodiv* (Petrén et al. 2023). This package considers the biochemical and structural diversity of the compounds present in a sample to calculate the overall chemodiversity per sample. First, we used the "calcDiv" function to calculate the functional Hill diversity index for each sample. Then we carried out an ANOVA test for the diversity indices, using a nested model of species nested within pollinator group to test for differences in chemodiversity.

Phylogenetic analyses of floral scent

To investigate the evolution of floral scent in a phylogenetic context we used a previously published phylogeny (Kay and Grossenbacher 2022). First, we trimmed the phylogeny to include only those species for which we have scent data using the "drop.tip" function in *ape* (Paradis and

Schliep 2018). To test for differences in the number of compounds produced by bee-pollinated and hummingbird-pollinated species while accounting for the phylogeny we carried out a phylogenetic anova using the "phylANOVA" function in *phytools* (Revell 2012).

To better understand how floral scent has evolved in the genus *Costus*, we carried out an ancestral state reconstruction of the number of compounds produced. We used the function "ace" in the *ape* package for ancestral character estimation (Paradis and Schliep 2018). We divided the compound number trait into twelve categories, each of which were assigned a different shade of blue. We plotted both the compound number for each phylogenetic tip label and internal node to illustrate how floral scent has evolved in *Costus*.

To test if floral scent shows phylogenetic signal in *Costus*, we used the multivariate generalization of Bloomberg's K (K_{mult}) (Adams 2014). Under Brownian motion, K_{mult} is expected to be 1. If $K_{mult}>1$, higher phylogenetic signal is detected than the null expectation under Brownian motion. If $K_{mult}<1$, lower phylogenetic signal is detected than the null expectation under Brownian motion. To calculate the K_{mult} of *Costus* floral scent, we used the filtered dataset with 1000 iterations to test significance. We carried out the analysis using the "physignal" function in the *geomorph* package (Adams and Otárola-Castillo 2013).

Sample collection for RNAseq

Costus allenii and *Costus villosissimus* were collected in Soberanía National Park, Colón Province, Panama. Vouchers are deposited at University of Panama (*Costus allenii*: 0132264, 0132265; *Costus villosissimus*: 0132270). *Costus lasius* was collected in El Valle de Antón, Cocle Province, Panama. Voucher is deposited in Michigan State University (MSC) herbarium Kay 0321. Permit 09-99. For all three species, the individuals used for RNAseq analyses were grown in greenhouses at UCSC. Flowers of each species were removed at approximately 9 am on the first day of flowering and flash frozen immediately in liquid nitrogen before being stored at -80°C until extraction.

RNA extraction and sequencing

Frozen flowers were removed and dissected on dry ice. Tissue from the petals and labella was broken down using a TissueLyser (Qiagen). RNA was then extracted using an RNeasy Mini Kit (Qiagen) with Qiashredder spin columns (Qiagen) following standard protocols. Samples

were sent to Novogene for quality control, library preparation, and sequencing. Our final dataset consisted of 19 samples: 8 *Costus allenii* (from 4 individual plants), 6 *Costus lasius* (from 2 individual plants), and 5 *Costus villosissimus* (from 1 individual plant). Samples were sequenced on a NovaSeq 6000 using 150 bp paired end reads. This generated approximately 53 million reads per library (mean=52.74 million, SD=12.01 million, N=19). The raw sequence data were deposited in the SRA under the BioProject accession PRJNA1010186.

Transcriptome assembly

Before assembling transcriptomes, we trimmed the raw reads using TrimGalore! (Martin 2011). We then assembled transcriptomes for each species using Trinity version 2.5.1 with default settings (Grabherr et al. 2011; Haas et al. 2013). To reduce redundancy, we clustered contigs with a minimum sequence identity of 95% using CD-HIT version 4.6.8 (Fu et al. 2012). We assessed transcriptome completeness and quality using BUSCO (v5.6.1) (embryophyta_odb10 dataset) (Simão et al. 2015; Manni et al. 2021; Zdobnov et al. 2021). We also checked assembly quality by mapping RNAseq reads back to the assembly using Bowtie (v2.4.1) to calculate mapping rates (Langmead and Salzberg 2012).

Terpene synthase gene expression analysis

We extracted the longest isoforms for each Trinity "gene" using the Trinity script "get_longest_isoform_seq_per_trinity_gene.pl" and translated these sequences. We then searched for potential TPSs using hmmsearch two HMM profiles: Terpene_syth_C (PF03936) and Terpene Synthase N-terminal domain (PF01397). We used the R package rhmmer to parse the output from hmmsearch resulting in a list of putative TPS sequences for each species. To reduce the TPSs to only those expressed in the dataset, we used a threshold of TPM>1 (transcripts per million) in at least one individual of a species (Eddy 2011; Arendsee 2017). To calculate expression of each putative TPS we normalized counts using Gene length corrected trimmed mean of M-values (GeTMM), an approach that improves inter- and intra-sample comparisons (Smid et al. 2018). To do this, we first calculated FPKM for each transcript and carried out TMM-normalization using the package *edgeR* (Robinson et al. 2010). We then combined GeTMM values for transcripts which were identified by Trinity to be the same gene. This does not normalize counts between species but is used to determine whether genes are lowly or highly expressed within a species.

Costus allenii genome assembly

We selected a wild-collected individual *C. allenii* from Pipeline Road, Soberanía National Park, Colón Province, Panama for *de novo* genome assembly. A voucher for this population of *C. allenii* is deposited at the University of Panama Herbarium (PMA:0132264). This individual was grown to flowering in the UCSC greenhouses from a cutting, and we harvested 1.5 g fresh tissue from leaf meristems and flower buds. We isolated cell nuclei following Workman (Workman et al. 2019) and then used the Circulomics Nanobind Plant Nuclei Big DNA kit to extract HMW DNA. We assessed DNA concentration with a Qubit Fluorometer (Thermo Fisher Scientific), purity with 260/280 and 260/230 absorbance ratios from a NanoDrop Spectrophotometer (Thermo Fisher Scientific) and ran a 7% agarose gel at 70 V for over 8 h to assess DNA fragment integrity and size. HMW DNA was sent to the UC Davis Genomics Center for additional cleaning, Pacific Biosciences HiFi library preparation, and sequencing on one PacBio Revbio SMRT cell. This produced 74.8 Gb of HiFi yield and 7.9 M HiFi reads. We assembled the PacBio data into a primary and alternative assembly using HiFiasm (v0.19.8)(Cheng et al. 2021). We then used RagTag (v2.1.0)(Alonge et al. 2022) to scaffold *C. allenii* contigs using the closely related *C. lasius* as a reference. We used D-GENIES (Cabanettes and Klopp 2018) with Minimap2 (Li 2018) to generate a dotplot comparing the two assemblies both before and after scaffolding. The genome assembly quality was assessed using BUSCO v 5.6.1 (Simão et al. 2015). Raw sequence data and the final genome assembly were submitted to NCBI under BioProject PRJNA1091680.

Genome annotations

Of the three species for which we generated RNAseq data, an unannotated genome was previously available for *C. lasius* (Harenčár et al. 2023). In this study we also generated a genome assembly for *C.allenii*. In addition, previously published genomes are available for both *C. bracteatus* and the more distantly-related *C. pulverulentus* (Valderrama et al. 2022; Harenčár et al. 2023). We started by processing RNAseq data as evidence for annotations. Trimmed reads from *C. lasius* were mapped using 2pass mapping in STAR to the *C. lasius* genome, and the *C. pulverulentus* genomes (Martin 2011; Dobin et al. 2013). Bam files were concatenated for use as described below. Trimmed reads from *C. allenii* were mapped using 2pass mapping in STAR to

both the *C. allenii* and the closely related *C. bracteatus* genomes, and bam files concatenated per species (Martin 2011; Dobin et al. 2013).

We annotated the genomes using BRAKER3 (v3.0.7) which combines RNA-seq and protein data in an automated pipeline (Lomsadze et al. 2005, 2014; Stanke et al. 2006, 2008; Gotoh 2008; Iwata and Gotoh 2012; Buchfink et al. 2015; Hoff et al. 2016, 2019; Kovaka et al. 2019; Brůna et al. 2020, 2021; Pertea and Pertea 2020; Gabriel et al. 2023). This pipeline requires a masked genome. We identified and annotated tandem repeats and transposable elements using RepeatModeler (Flynn et al. 2020) (v.2.0.4 for *C. lasius* and v.2.0.5 for the other genomes) and RepeatMasker v.4.1.5 (Tarailo-Graovac and Chen 2009). We then used RepeatMasker with the outputs of RepeatModeler to generate softmasked genomes. The masked genomes were then provided to BRAKER along with plant proteins downloaded from OrthoDB (odb10_plants) (Zdobnov et al. 2021). For all species, BRAKER was run in ETP mode which combines evidence from both proteins and RNAseq (Gabriel et al. 2021). BUSCO v 5.6.1 (Simão et al. 2015) and OMArk (Nevers et al. 2022) were used to evaluate the completeness and consistency of the sets of gene models.

Terpene synthase gene family annotation

Following whole-genome annotation, we manually curated the gene models for terpene synthase (TPS) genes in the annotation. To do this, we used bitacora (Vizueta et al. 2020), a pipeline which curates an existing annotation and finds additional gene family members. In this pipeline, BLASTP and hmmer are used to search for gene family members of interest within the existing annotation (Altschul et al. 1990; Eddy 2011). Additional regions of the genome are then searched using TBLASTN and are annotated using GeMoMa (Keilwagen et al. 2019). Hmmer is used to validate the gene models. As input, we used two HMM profiles: Terpene_syth_C (PF03936) and Terpene Synthase N-terminal domain (PF01397) downloaded from Pfam. In addition, we provided previously annotated genes from *Arabidopsis thaliana* and *Oryza sativa* (Chen et al. 2011; Yu et al. 2020; Jia et al. 2022). Gene models from bitacora and the genome-wide annotation from BRAKER were compared and TPS genes were manually curated using IGV (Robinson et al. 2011). We also searched for additional TPSs by carrying out exonerate searches using the curated *Costus* gene models (Slater and Birney 2005). We checked all

annotated TPSs for complete protein domains using the NCBI conserved domain search (Marchler-Bauer et al. 2015). We excluded proteins with less than 250 amino acids.

Gene family analysis

The *Costus* TPS protein sequences, combined with those from *A. thaliana*, were aligned with MAFFT v7.508 (-maxiterate 1000, using L-INS-I algorithm) (Katoh and Standley 2013). We then trimmed the alignment using trimAl (-gt0.6, sites only included when present in 60% of sequences) (Capella-Gutierrez et al. 2009). We used this alignment to construct a gene tree with IQ-TREE and the ModelFinder function to determine the best-fit model (Nguyen et al. 2015; Kalyaanamoorthy et al. 2017; Hoang et al. 2018). We rooted the tree using the *phytools* package in R ("midpoint.root" function)(Revell 2012; R Core Team 2023). We plotted the resulting gene trees using the following packages in R: *ape* (Paradis and Schliep 2018), *evobiR* (Blackmon and Adams 2015), *ggnewscale* (Campitelli 2023), *ggstar* (Xu 2022), *ggtree* (Yu et al. 2017), *ggtreeExtra* (Xu et al. 2021), and *tidytree* (Yu 2022).

Differential expression analyses

First, we trimmed the reads using TrimGalore! (Martin 2011). We then mapped the reads from all three species to both the *Costus allenii* and *Costus lasius* genome (Harenčár et al. 2023). We ran 2pass mapping using STAR (Dobin et al. 2013). In general, we found higher levels of multi-mapped *C. allenii* reads when mapped to *C. allenii*. To investigate this we used mmquant (with merge, -m, set to 10) to count the reads, a tool which can account for multi-mapping reads (Zytnicki 2017). The output from mmquant was read into R for further analysis. To calculate percentage of gene expression due to TPS expression, we normalized reads by library size using TMM (trimmed mean of M values) (Robinson and Oshlack 2010). Due to the consistency in TPS expression as calculated by mapping to both genomes, we decided to use the *C. lasius* genome assembly to identify genes differentially expressed between the three species to remove the complication of multi-mapping. To do this, we first counted reads using featureCounts (Liao et al. 2014) and again read the output into R. We filtered genes to include those with at least one count per million (CPM) in at least one library and normalized reads by library size using TMM (trimmed mean of M values). Differential gene expression was evaluated using the non-parametric "noiseqbio" function from the *NOISeq* package (Tarazona et al. 2011, 2015). We

used the default cut-off of q=0.95 in the "degenes" function which is equivalent to an adjusted p-value of 0.05.

GO Analysis

We functionally annotated *C. alennii* genes using Blast2GO (Götz et al. 2008; Burge et al. 2012). We imported these functional annotations into R to carry out enrichment analysis with the package *topGO* (Alexa and Rahnenfuhrer 2022). We considered the background to be all genes included in that specific differential expression analysis after filtering.

Plotting and data manipulation

Additional packages used for general plotting: *cowplot* (Wilke 2020), *ggplot2* (Wickham 2009), and *scico* (Pedersen and Crameri 2023). Packages used for data transformation and manipulation include: *data.table* (Barrett et al. 2024), *dplyr* (Wickham et al. 2021), *knitr* (Xie 2023), *magrittr* (Bache and Wickham 2023), *readr* (Wickham et al. 2023), *reshape2* (Wickham 2007), and *tibble* (Müller and Wickham 2022). Analyses were carried out in R version 4.3.2 (R Core Team 2023).

Results

Bee-pollinated species produce more compounds and more diverse floral scents

We collected 101 samples from 29 *Costus* species including both bee- and hummingbird-pollinated species. Using multivariate techniques, we visualized the floral scent profiles both before and after filtering for floral scent compounds to identify the broad patterns in our dataset. Before filtering our data, we found that samples from hummingbird-pollinated species did not differ from ambient samples (Fig S1A). In contrast, samples from bee-pollinated species spread across a wider section of chemospace, with many samples visually separated from both ambient and hummingbird-pollinated samples (Fig. S1A). We found that both pollination group, and species (nested within pollination group) explained variation in floral scent (PERMANOVA, pollination group: $F_{3,168}=5.6$, $p<0.001$; species: $F_{27,168}=2.5$, $p<0.001$). Interestingly, bee-pollinated species were significantly different from both hummingbird-pollinated species and ambient samples (Pairwise PERMANOVA, p=0.006), whereas hummingbird-pollinated species

did not differ from ambient samples (Pairwise PERMANOVA, p=0.084) (Figure S1A). This pattern held true for the relative abundance dataset (Figure S2A).

After filtering likely contaminants, we obtained a final dataset with 60 floral scent compounds. By removing the ambient compounds, we found that one bee-pollinated sample, one hybrid sample, and eighteen hummingbird-pollinated samples had no detectable floral scent and so were removed from the dataset to facilitate visualization using NMDS. When this filtered dataset was plotted, we observed more overlap between the hummingbird- and bee-pollinated samples, but the two sets of samples significantly different (PERMANOVA, pollination group: $F_{2,100}$=5.8, p<0.001; species: $F_{27,100}$=2.6, p<0.001; Pairwise PERMANOVA bee- vs hummingbird-pollinated species p=0.003) (Figure 1B). This pattern held true for the relative abundance dataset (Figure S2B).

To see how individual compounds varied between bee- and hummingbird-pollinated species we calculated the percentage of individuals in each pollination group which produced the most common floral scent compounds in the dataset. We found that these compounds are found in a higher proportion of bee-pollinated flowers than hummingbird-pollinated flowers (Fig. 1). In particular, beta-Ocimene and beta-Caryophyllene show the largest percentage differences between the two pollination groups (Fig.1).

Overall, bee-pollinated flowers produced more floral scent compounds, averaging 9 (s.d. 10) compounds in comparison to only 2 (s.d. 4) for hummingbird-pollinated flowers. Bee-pollinated flowers contained more compounds than hummingbird-pollinated flowers (Fig 2A). In addition, the bee-pollinated floral scents had a higher chemical diversity (Fig 2B).

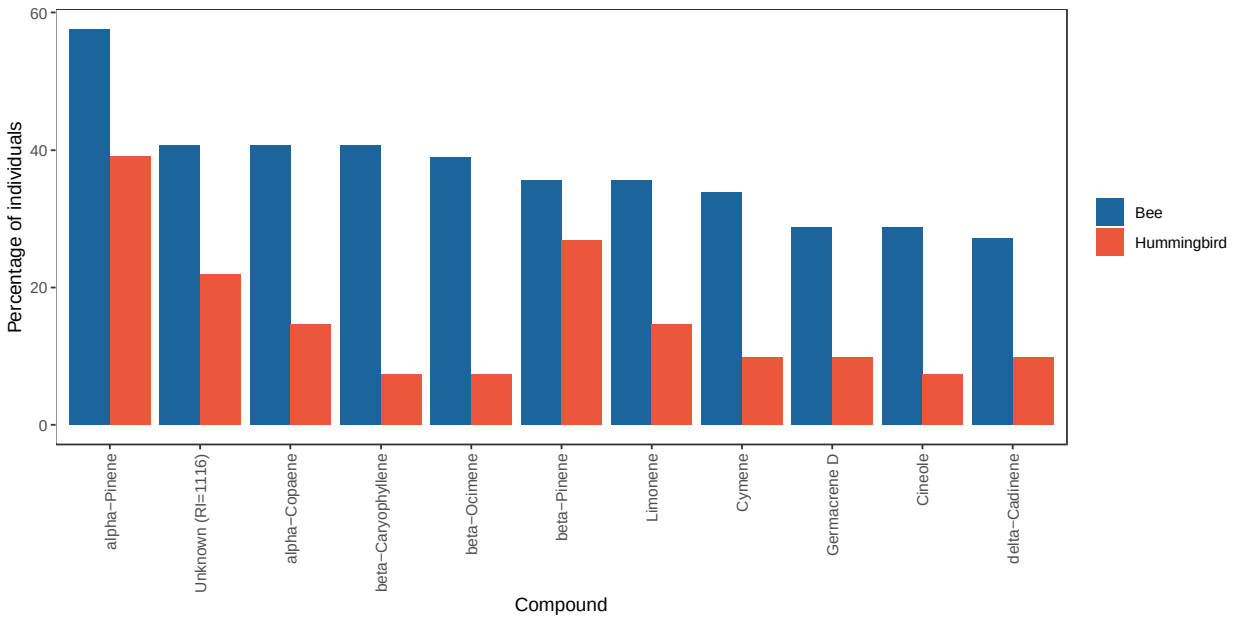

Figure 1 Bar plot showing percentage of individuals of bee-pollinated and hummingbird-pollinated flowers that produced the most common floral scent compounds in the dataset.

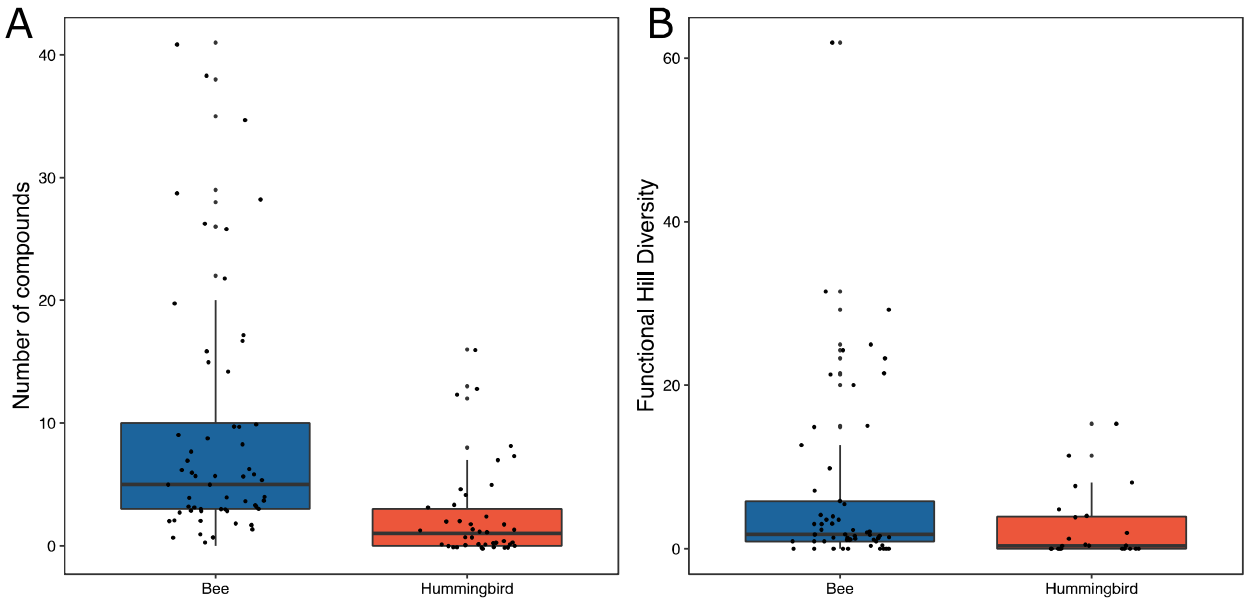

Figure 2. Boxplots highlighting differences in bee-pollinated and hummingbird-pollinated *Costus* species in terms of A) Number of scent compounds produced (ANOVA, pollination group: $F_{1,71}$=58.6, p<0.0001, species: $F_{27,71}$=9.7, p<0.0001) and B) The diversity of scent compounds produced (ANOVA, pollination group: $F_{1,53}$=5.0, p=0.03, species: $F_{25,53}$=3.0, p=0.0003).

Ancestral state reconstructions show that hummingbird-pollinated species have lost floral scent

To understand the evolution of floral scent in *Costus*, we carried out phylogenetic analyses. To confirm our previous result, we tested for differences in compound number produced by bee- and hummingbird-pollinated species accounting for phylogeny. We found that, as in our previous results, bee-pollinated species produce significantly more floral scent compounds (Phylogenetic ANOVA, F=6.7, p=0.049). We also tested for evidence of phylogenetic signal in floral scent, detecting weak and non-significant phylogenetic signal overall (Kmult=0.43, p=0.677).

To further investigate how floral scent has evolved across the *Costus* phylogeny, we carried out maximum likelihood ancestral state reconstruction. The ancestral state of all *Costus* species found in tropical America is to produce more compounds than average hummingbird-pollinated species (4.5 vs 2). In this reconstruction, the ancestral *Costus* population produced an average floral scent – more compounds than hummingbird-pollinated species but less than the average bee-pollinated species (Figure 3). Many hummingbird-pollinated species have since completely lost floral scent, as shown by the white circles (Figure 3). In contrast, some bee-pollinated species have evolved much stronger floral scents than the ancestral state, such as *Costus allenii*.

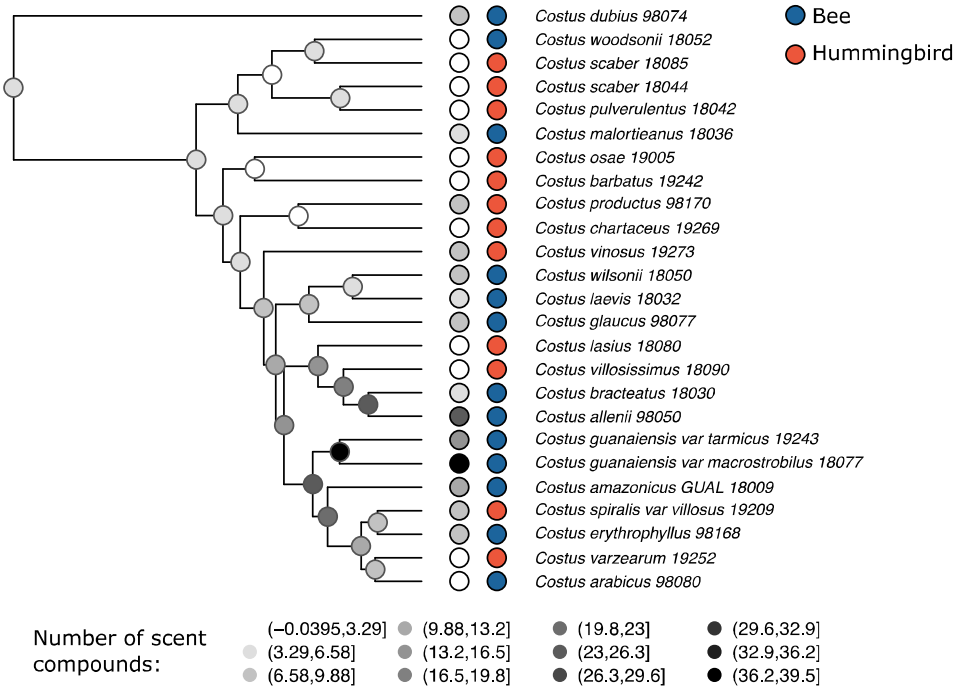

Figure 3. Ancestral state reconstruction including of floral scent in the genus *Costus*. Pollinator for each species is illustrated by the right-hand dots. Compound number for each species is shown by the left-hand dots with darker dots representing more compounds being produced. Predicted compound production at each node is shown following the same color scale. Tip labels are the same as those used in (Vargas et al. 2020).

<u>Loss of floral scent is correlated with downregulation of floral terpene synthase genes.</u>

To analyze the genetic basis of floral scent evolution, we first needed to choose a clade of closely related species with variation in floral scent production. We chose the clade containing *Costus lasius* due to the variation in floral scent production and the availability of a high-quality genome. In this clade, *Costus lasius* (hummingbird-pollinated) produces on average three floral scent compounds, while *Costus allenii* (bee-pollinated) produces 24 (one of the highest in our dataset), and *Costus villosissimus* (bee-pollinated) produces seven compounds (Figure 4A).

We first produce transcriptome assemblies of all three species. After clustering transcripts with over 95% similarity, we found 112998 transcripts present in *C. allenii*, 80208 in *C. lasius*, and 96886 in *C. villosissimus*. Re-mapping rates were high in all three species: 99.2% in *C. allenii*, 99% in *C. lasius*, and 99.1% in *C. villosissimus*. All three also had BUSCO scores of more than 80% (Table S2). We then extracted TPS sequences from these transcriptomes for further analyses.

We found that 20 TPS genes were expressed in *C. allenii*, compared to five in *C. villosissimus*, and only one in *C. lasius*, when expression was defined as one TPM in at least one sample of the species. Furthermore, we found that counts of TPS expression per TPS gene expressed were much higher in both *C. allenii* and *C. villosissimus* when compared to *C. lasius* (Fig. 4B). In fact, in *C. allenii*, a TPS is the highest expressed gene in the transcriptome, and TPSs are also the 4th and 6th most expressed genes in the transcriptome, highlighting the extent of expression. On average, 12% of total expression can be attributed to TPSs in *C. allenii*, 0.17% in *C. villosissimus* and 0.00014% in *C. lasius*, highlighting the orders of magnitude differences

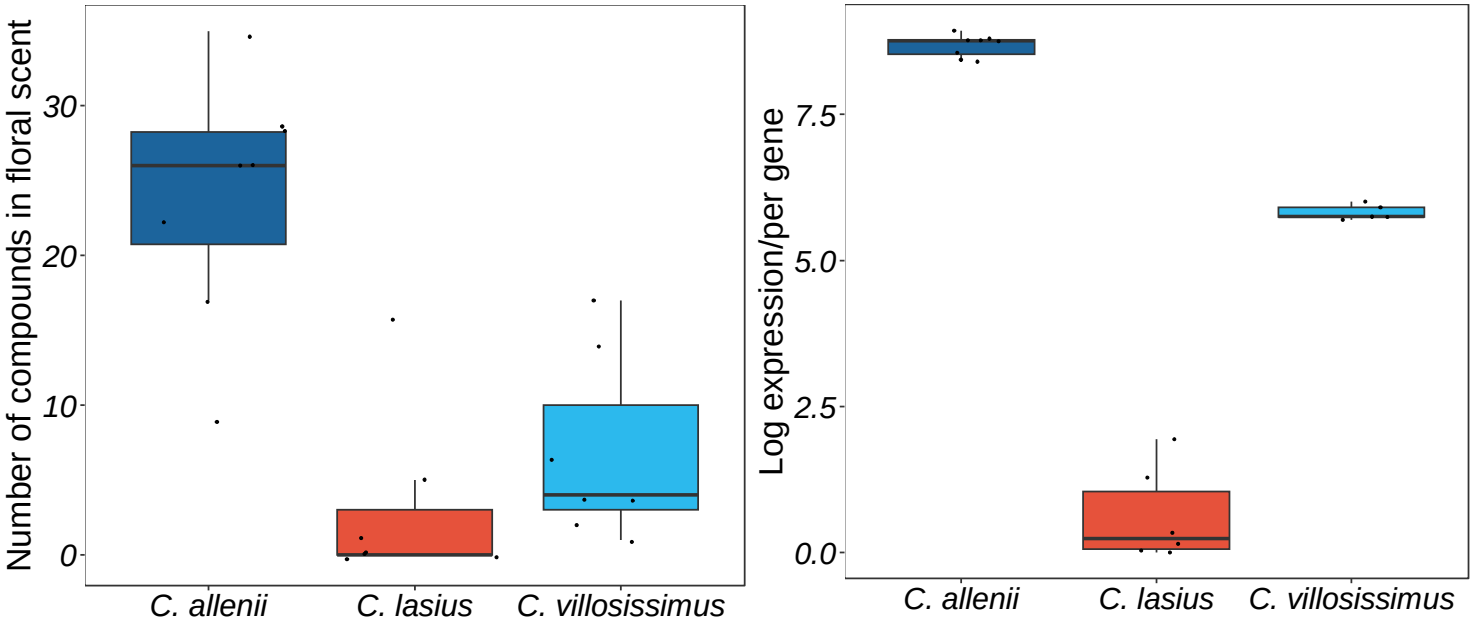

between species.

Figure 4. Differences in floral scent and gene expression between *C. allenii*, *C. lasius*, and *C. villosissimus*. Species differ significantly in A) number of compounds found in floral

scent (ANOVA, $F_{2,19}$=20.1, p<0.001), and (B) expression of terpene synthase transcripts (ANOVA, $F_{2,16}$=508.4, p<0.001).

Floral scent loss is not driven by gene loss in *Costus*

While the transcriptome assemblies can give us an insight into levels of TPS expression, it is hard to determine gene copy number due to the redundancies in the assemblies. For this, we need genome data to allow us to determine the number of TPS genes in each species. There are currently three publicly available *Costus* genomes: *C. bracteatus* (bee), *C. lasius (hummingbird)*, and *C. pulverulentus* (hummingbird) (Valderrama et al. 2022; Harenčár et al. 2023). We assembled a reference genome for *C. allenii* (bee) to generate a dataset of two hummingbird- and two bee-pollinated species. The assembled *C. allenii* genome was 1.1Gb, with a corresponding N50 value of 120Mb. Over half of the total assembly was contained in the 5 longest scaffolds (L50=5)(Table S3). We used BUSCO to assess genome assembly completeness using the embryophyte dataset. Of the 1614 core genes searched, we found 98.8% (1594) in our assembly. Of these, 90.8% (1465) were single-copy, 8% (129) duplicated and 0.3% (5) fragmented, highlighting the high quality of our final assembly.

We annotated between 63-75% of each genome as repeat elements (Tables S4, S5, S6, S7) . We found that, of the elements that could be classified, retrotransposable elements represented the largest percentage of the genome. These are the most abundant form of repeat elements found in angiosperm genomes. Many repeats were not classified into previously known families, perhaps suggesting the existence of new repeat elements.

A pipeline combining de novo prediction and homology-based prediction methods was used to generate protein-coding gene models for each genome. We annotated 28,442 genes in *C. allenii*, 27,794 in *C. bracteatus*, 28,409 in *C. lasius*, and 26,696 in *C. pulverulentus*. We evaluated annotation completeness using the Embryophyta database in BUSCO, with over 90% complete for all annotations (Table 1). We further assessed annotation quality using OMArk, which assesses both completeness and consistency of the annotation when compared to closely related species. Using the commelinid database, OMArk found a high percentage of orthologous groups were present in the annotations (*C. allenii* 88% (9847/11155), *C. bracteatus* 87% (9685/11155), *C. lasius* 88% (9826/11155), *C. pulverulentus* 87% (9758/11155)). Furthermore, a high percentage of the proteome for each species was assessed as having consistent lineage

placement (*C. allenii* 86%, *C. bracteatus* 87%, *C. lasius* 86%, *C. pulverulentus* 87%). No contamination was detected. Overall, the generated annotations were of high quality for all genomes.

Table 1. BUSCO scores for annotations searched against the Embryophyta database.

	C. allenii	*C. bracteatus*	*C. lasius*	*C. pulverulentus*
Complete	1493 (92.5%)	1457 (90.2%)	1480 (91.7%)	1466 (90.9%)
Complete and single copy	1139 (70.6%)	1116 (69.1%)	1121 (69.5%)	1152 (71.4%%)
Complete and duplicated	354 (21.9%)	341 (21.1%)	359 (22.2%)	314 (19.5%)
Fragmented	12 (0.7%)	25 (1.5%)	19 (1.2%)	21 (1.3%)
Missing	109 (6.8%)	132 (8.3%)	115 (7.1%)	127 (7.8%)
Total searched	1614	1614	1614	1614

We annotated a total of 66 TPSs in *C. allenii*, 44 in *C. bracteatus*, 40 in *C. lasius*, and 44 in *C. pulverulentus*. To classify these TPSs in previously described TPS families, we constructed a phylogenetic tree based on amino acid sequences with TPSs from *Arabidopsis thaliana*. All TPSs belonged to the families TPS-a, TPS-b, TPS-c, TPS-e/f, and TPS-g (Fig. 5). While we did not see evidence for gene loss in the hummingbird-pollinated species, we see lineage-specific gene duplications in *C. allenii*, the species which produces the most diverse floral scent in our dataset.

We mapped the RNAseq reads both to the *C. allenii* genome and the *C. lasius* genome. In *C. allenii*, we found a consistent percentage of successfully mapped reads attributed to TPSs as with the transcriptome (12% transcriptome, 13% mapped to either genome). We found some differences for both *C. lasius* and *C. villosissimus*. For the *C. villosissimus* transcriptome mapping, we found 0.17% of reads were attributed to TPSs, in comparison to 0.009% when mapped to either genome. Due to a lack of genome for *C. villosissimus*, it is unclear whether this could be due to genetic changes or rearrangements not captured by the available genomes. For *C. lasius*, we found only 0.00014% of reads mapped to the transcriptome were due to TPSs, in contrast to 0.011% of the genome-mapped reads. This could be due to non-protein coding transcripts in the transcriptome diluting the TPS count.

When *C. allenii* reads were mapped to the *C. allenii* genome, we found high levels of multi-mapping. This is due to recent TPS duplications in *C. allenii* which are highly expressed. To illustrate this, the highest gene expressed in *C. allenii* is *TPS49*, and the third most expressed "gene" consists of reads that multimap to *TPS49* and *TPS52*. This clade is represented by only one gene in each of the other species. Other recent lineage-specific duplications include *TPS2*, *TPS3*, *TPS4*, and *TPS5* where the majority of reads multimap due to sequence similarity between duplicates. Both of these clades have only one member in each of the other species with a genome (Fig S3). This highlights the complexity of mapping to gene families with recent duplications, especially when they are highly expressed, meaning that ignored multi-mapped reads will lose large percentages of mapped reads. We, therefore, decided to carry out our differential expression analysis using the *C. lasius* genome.

By mapping all reads to the *C. lasius* genome, we identified 4790 genes differentially expressed between *C. allenii* and *C. lasius*, 7678 between *C. allenii* and *C. villosissimus*, and 6191 between *C. lasius* and *C. villosissimus*.Of the 40 TPS genes found in the *C. lasius* genome, 15 were differentially expressed between *C. allenii* and *C. lasius*, with 13 of these upregulated in *C. allenii*. This includes *TPS33*, orthologous to the *TPS49*/*52* clade, the most highly expressed genes in *C. allenii*. We found 19 TPSs that were differentially expressed between *C. allenii* and *C. villosissimus*, with 14 upregulated in *C. allenii* and 5 in *C. villosissimus*. Ten TPS genes were differentially expressed between *C. lasius* and C. *villosissimus*, with 7 upregulated in *C. villosissimus* and 3 in *C. lasius*. Overall, more TPSs were upregulated in *C. allenii* when compared to either *C. lasius* or *C. villosissimus*. Our gene ontology analysis found little evidence for functional enrichment in differentially expressed genes between species (Table S8).

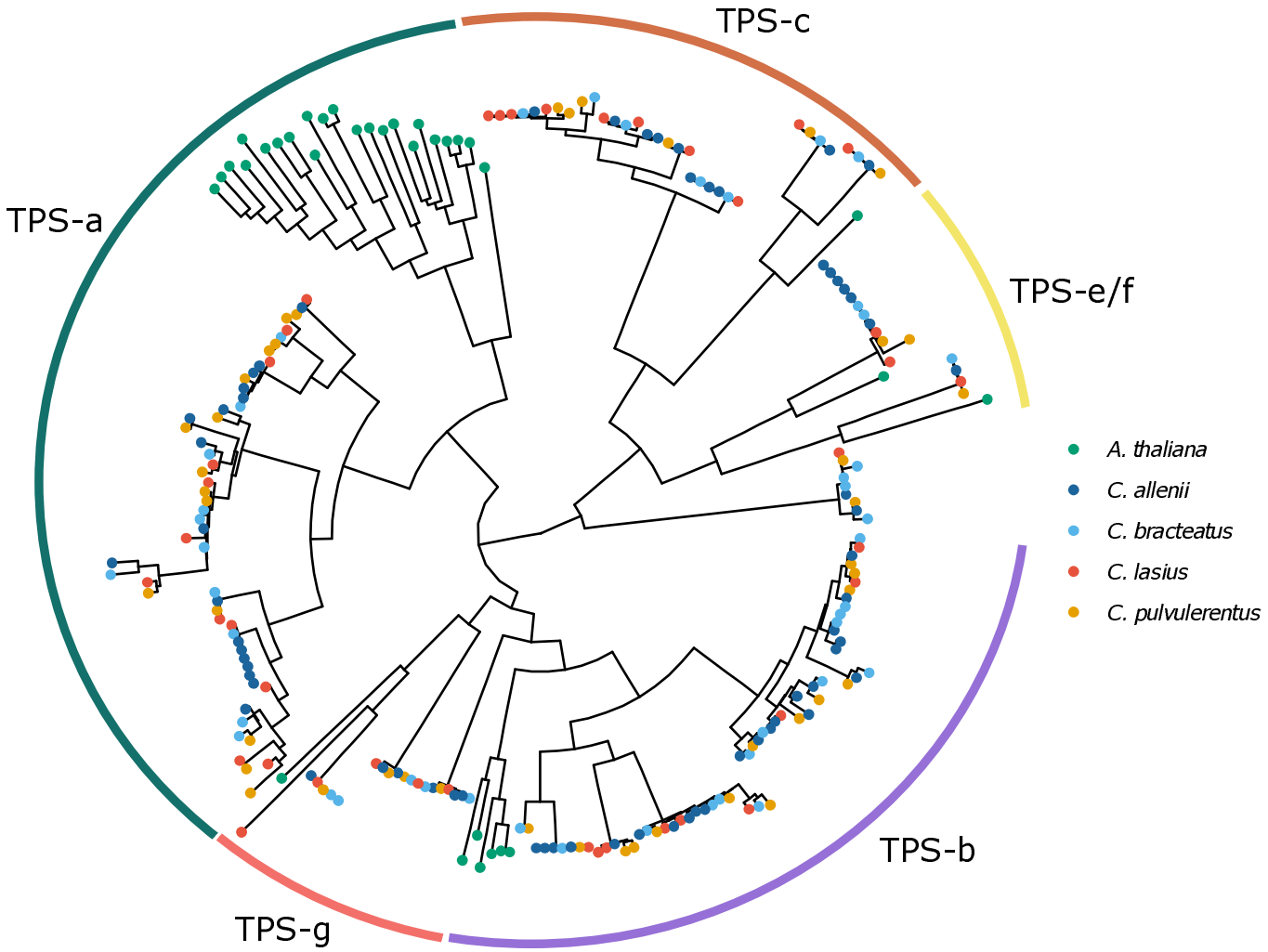

Figure 5. Phylogenetic analysis of terpene synthase gene families. The phylogeny was constructed in IQ-TREE with 1000 bootstraps and model LG. TPS family classifications based on *Arabidopsis thaliana* are illustrated.

Discussion

Repeated evolutionary transitions provide unique opportunities to study the extent of convergence both at the phenotypic and molecular level, shedding light on the predictability of evolution. Transitions to hummingbird pollination are widespread in the Americas and are predicted to be associated with loss of floral scent, however, this has not been studied in a

comparative framework across multiple independent transitions within the same genus. In this study, we combine comparative chemical ecology with genomics and transcriptomics and demonstrate that floral scent evolution in the genus Costus is highly associated with pollinator type. We found that hummingbird-pollinated *Costus* species have lost their floral scent, or produce a greatly reduced scent, whereas bee-pollinated species in the Americas exhibit either maintenance of floral scent or gain of a more diverse scent profile. We find that this is related to downregulation of genes associated with floral scent production (in this case terpene synthases) in floral tissues of hummingbird-pollinated species but is not accompanied by loss of terpene synthase genes.

We found that hummingbird-pollinated species produced little to no floral scent. In contrast, the bee-pollinated species showed much greater variation with some species having extremely diverse floral scents, yet others producing far fewer compounds. Bee-pollinated species also show greater morphological variation, possibly reflecting variation in orchid bee diversity (Kay and Grossenbacher 2022). Furthermore, not all species in our dataset follow the expected patterns. *Costus arabicus* (bee-pollinated) produces less floral scent than the closely related *C. erythrothyrsus* (hummingbird-pollinated). *Costus vinosus* (bee-pollinated) also produces little scent. It is unclear whether the variation in floral scent between different bee-pollinated species is related to pollinator preference, other abiotic or biotic factors, or historical contingency.

There are multiple hypotheses for why floral scent would be lost in hummingbird-pollinated species. Firstly, it could be because there is simply no selection to maintain the production due to poor sense of smell, or lack of preference shown for floral scent, by hummingbirds (Bang and Cobb 1968; Goldsmith and Goldsmith 1982; Knudsen et al. 2004; Driver and Balakrishnan 2021). If this were the case, we might expect to find a correlation between length of time following pollinator transition and extent of floral scent loss. However, our data shows that downregulation of floral scent can occur on relatively quick evolutionary timescales. *Costus wilsonii*, *C. lasius*, and *C. spiralis*, are all hummingbird-pollinated species that are most closely related to bee-pollinated species, representing more recent evolutionary shifts to hummingbird pollination. Yet all three species produce little to no floral scent, suggesting there can be quick breakdown of floral scent production following pollinator transitions. This observation is consistent with previous studies that have shown that floral scent

often evolves rapidly in response to selection (Ramos and Schiestl 2019; Zu et al. 2020; Liu et al. 2024).

The rapid and repeated scent loss in hummingbird-pollinated species suggests a shared strong selection pressure against floral scent production. One potential reason for this could be due to the energetic cost of producing terpenes. A similar argument has been made in the case of eye regression in cavefish. If vision is energetically costly then it should be selected against when no longer useful (Moran et al. 2015; Sifuentes-Romero et al. 2023). This is supported by evidence of the energetic costs of the visual system (Moran et al. 2015). For terpene metabolism this cost is unknown, and is thought to be minimal (Raguso 2016; Pichersky and Raguso 2018). In fact, it has been argued that the complex network of terpene metabolism with enzymes producing multiple different products makes it more efficient, without the need for a separate enzyme and regulator for each step as in a linear pathway (Lanier et al. 2023).

Alternatively, it could be that instead of energetic costs, terpene production has ecological costs for hummingbird-pollinated species, for example, strong selection against bee attraction (Castellanos et al. 2004; Bergamo et al. 2016). Many benefits to hummingbird pollination have been described. Birds do not groom and consume pollen leading to less pollen loss, birds can travel longer distances between plants, and birds can promote more gene flow, which is beneficial to combat inbreeding depression in species (Thomson and Wilson 2008; Krauss et al. 2017; Dellinger et al. 2022). One caveat is that comparisons in pollination effectiveness between bees and hummingbirds have not been carried out in orchid bees which tend to forage over long distances, perhaps resulting in a more “bird-like” gene flow (Janzen 1971, 1981; Opedal et al. 2017; Kay and Grossenbacher 2022; Gamba and Muchhala 2023). A final piece of evidence to support this is the large reduction in beta-ocimene production in hummingbird-pollinated flowers relative to bee-pollinated flowers as this compound is a common pollinator attractant (Farré-Armengol et al. 2017). In *Mimulus*, loss of monoterpenes, including beta-ocimene, maintain reproductive isolation between bee- and hummingbird-pollinated mimulus species (Byers et al. 2014). While pollinator efficiency is unknown in *Costus*, rapid floral scent loss supports the hypothesis of “bee-avoidance” following establishment of hummingbird pollination.

We found that the floral scents of *Costus* are dominated by terpene compounds. Terpene diversity in a given organism is mainly determined by the terpene synthase (TPS) gene family, which carry out crucial steps in terpene formation (Tholl 2006). Neither hummingbird-pollinated species with a genome (*C. lasius* and C. *pulverulentus*) exhibited loss of TPS genes. There are multiple reasons why trait loss would be associated with changes in gene regulation rather than gene loss. Firstly, these cases may represent recent transitions to hummingbird pollination and that at least some of these TPSs that were responsible for floral scent production will eventually be lost. This has been proposed as a "step-wise" model to pseudogenization, whereby reduction in expression is followed by relaxed selection and then loss-of-function mutations, as seen in an enzyme lost in marine mammals (Graham et al. 2023).

Alternatively, we might not expect any TPS genes to be lost even in the long term. Terpenes, and therefore TPSs, are important for many other roles in plants. Plants use terpenes to deter herbivores, to attract parasitoids or predators of herbivores, and as anti-fungal and anti-bacterial compounds to prevent disease (Gershenzon and Dudareva 2007). These pleotropic functions of TPSs could explain why we observe downregulation in floral tissues specifically rather than any pseudogenization. One argument against this is that in other systems TPS pseudogenization does occur following pollinator transitions. In *Mimulus*, loss of monoterpene production (specifically beta-ocimene), is not due to expression differences but loss-of-function mutations (Peng et al. 2017). It is unclear whether pseudogenization will occur at some point in *Costus*.

Although we did not observe gene loss in hummingbird-pollinated lineages, we did observe extensive lineage-specific duplications in the bee-pollinated species *C. allenii*. *Costus allenii* was one of the species with highest scent diversity in our dataset, and we found multiple TPS genes to exhibit several recent lineage-specific duplication events. We also found extremely high TPS expression, accounting for approximately 12% of expression in floral tissue. The gene with the highest expression in floral tissue was found to be a TPS-a family member, with high expression also found also for several TPS-b members. These two families produce sesquiterpenes and monoterpenes, respectively, both of which are found in the floral scent of *C. allenii*. In *C. lasius* and *C. villosissimus*, we found reduced TPS expression compared to *C. allenii*, as expected based off their reduced floral scent production. We also saw high levels of phenotypic variation in *C. villosissimus*, and there is no publicly available genome, making

interpretation of the results more difficult. While the overall trends are clear, we hesitate to over-interpret the gene expression data as we have only sampled at one timepoint (first day of flowering) and it is possible that there is floral scent production happening earlier that is not captured in our data.

We observe more consistency and predictability in the phenotypic patterns than the underlying molecular mechanisms. In many systems, parallel changes in floral scent have accompanied independent pollinator shifts, including the current study (Knudsen et al. 2004; Byers et al. 2014). This can also be seen in other reproductive shifts, such as transitions to self-fertilization (Wozniak et al. 2022). In some systems, the underlying molecular mechanisms of floral scent loss are also convergent, having been shown to involve the same loci in multiple independent evolutionary events. For example, loss of floral scent in different *Mimulus* lineages is due to changes at the same loci, including frameshifts, deletions, and potentially post-transcriptional regulation (Peng et al. 2017). A similar pattern was found in two different systems that have lost benzaldehyde floral scent production due to either evolution of self-fertilization (Sas et al. 2016), or hummingbird pollination (Amrad et al. 2016). The same loci contains loss-of-function mutations in both cases (Raguso 2016). However, this is not universally true. In *Capsella*, the loss of beta-ocimene following transition to self-fertilization in one lineage is due to changes in subcellular enzyme localization, but QTL results suggests another loci is responsible for scent loss in a related species (Wozniak et al. 2022). In this study, we saw no evidence for pseudogenization. Instead, we found evidence that gene expression differences are responsible for scent differences between *Costus* species, with scent loss likely due to changes in, potentially tissue-specific, gene expression.

In summary, we have shown that *Costus* species exhibit repeated loss of floral scent following transitions from bee to hummingbird pollination suggested a shared strong selection pressure favoring scent loss. We also find bee species that have recently gained incredibly diverse scents, which, at least in *C. allenii*, is associated with lineage-specific terpene synthase duplications. We show that scent loss is not associated with loss of terpene synthase genes but rather appears to be due to gene downregulation. This demonstrates the capacity for rapid metabolic changes in response to selection following pollinator transitions. This system provides us with the exciting opportunity to identify the cis- or trans-regulatory changes driving gene

expression differences in multiple independent transitions to hummingbird pollination, allowing us to study the extent of genetic convergence in this system.

Acknowledgements

This work was funded by the National Science Foundation Dimensions of Biodiversity grant awarded to K.M.K. (DEB-1737889) and S.R.R. (DEB-1737771), and the Jean H. Langenheim Chair in Plant Ecology and Evolution held by K.M.K. We thank the Organization for Tropical Studies, Estación Biológica Monteverde, and Estación Tropical La Gamba for facilitating field work in Costa Rica and the Smithsonian Tropical Research Institute for facilitating field work in Panama. All field research was conducted with appropriate research permits in Costa Rica (M-P-SINAC-PNI-ACAT-026-2018, ACC-PI-0272018, MPC-SINAC-PNI-ACLAP-020-2018, INV-ACOSA-076-18, MPC-SINAC-PNI-ACTo-020-18, CONAGEBIO R-056-2019OT and R-058-2019-OT) and Panama (SE/AP-13-19, 09-99) We thank J. Harenčár for assistance with lab work, P. Juarez for assistance with field sampling, and Alyssa Kaatmann, Aubrie Tait, Kate Uckele, Melina Sauerman Carrizosa, and Selena Vengco for assistance with greenhouse sampling. We thank J. Velzy and S. Childress for greenhouse care of the UCSC living Costus collection. We thank the Ramírez lab for helpful discussions.

Author Contributions

Conceptualization, K.D., K.M.K., and S.R.R.; Investigation, K.D. and K.M.K.; Formal Analysis, K.D.; Visualization, K.D.; Resources, K.M.K. and S.R.R.; Writing – Original Draft, K.D.; Writing – Review and Editing, K.D., K.M.K., and S.R.R.; Supervision, K.M.K. and S.R.R.; Project Administration, K.M.K. and S.R.R.; Funding Acquisition, K.M.K. and S.R.R.

References

Abrahamczyk, S., and S. S. Renner. 2015. The temporal build-up of hummingbird/plant mutualisms in North America and temperate South America. BMC Evol. Biol. 15:104.

Adams, D. C. 2014. A generalized K statistic for estimating phylogenetic signal from shape and other high-dimensional multivariate data. Syst. Biol. 63:685–697.

Adams, D. C., and E. Otárola-Castillo. 2013. geomorph: an r package for the collection and analysis of geometric morphometric shape data. Methods Ecol. Evol. 4:393–399.

Albert, V. A., S. E. Williams, and M. W. Chase. 1992. Carnivorous Plants: Phylogeny and Structural Evolution. Science 257:1491–1495. American Association for the Advancement of Science.

Alexa, A., and J. Rahnenfuhrer. 2022. topGO: Enrichment Analysis for Gene Ontology.

Alonge, M., L. Lebeigle, M. Kirsche, K. Jenike, S. Ou, S. Aganezov, X. Wang, Z. B. Lippman, M. C. Schatz, and S. Soyk. 2022. Automated assembly scaffolding using RagTag elevates a new tomato system for high-throughput genome editing. Genome Biol. 23:258.

Amrad, A., M. Moser, T. Mandel, M. de Vries, R. C. Schuurink, L. Freitas, and C. Kuhlemeier. 2016. Gain and Loss of Floral Scent Production through Changes in Structural Genes during Pollinator-Mediated Speciation. Curr. Biol. 26:3303–3312.

Arendsee, Z. 2017. rhmmer: utilities parsing “HMMER” results.

Bache, S. M., and H. Wickham. 2023. magrittr: A Forward-Pipe Operator for R.

Bang, B. G., and S. Cobb. 1968. The Size of the Olfactory Bulb in 108 Species of Birds. The Auk 85:55–61. American Ornithological Society.

Barrett, T., M. Dowle, A. Srinivasan, J. Gorecki, M. Chirico, and T. Hocking. 2024. data.table: Extension of `data.frame`.

Bergamo, P. J., A. R. Rech, V. L. G. Brito, and M. Sazima. 2016. Flower colour and visitation rates of *Costus arabicus* support the 'bee avoidance' hypothesis for red-reflecting hummingbird-pollinated flowers. Funct. Ecol. 30:710–720.

Blackmon, H., and R. A. Adams. 2015. EvobiR: Tools for comparative analyses and teaching evolutionary biology. , doi: 10.5281/zenodo.30938.

Burge, S., E. Kelly, D. Lonsdale, P. Mutowo-Muellenet, C. McAnulla, A. Mitchell, A. Sangrador-Vegas, S.-Y. Yong, N. Mulder, and S. Hunter. 2012. Manual GO annotation of predictive protein signatures: the InterPro approach to GO curation. Database J. Biol. Databases Curation 2012:bar068.

Byers, K. J. R. P., H. D. Bradshaw, and J. A. Riffell. 2014. Three floral volatiles contribute to differential pollinator attraction in monkeyflowers (*Mimulus*). J. Exp. Biol. 217:614–623.

Cabanettes, F., and C. Klopp. 2018. D-GENIES: dot plot large genomes in an interactive, efficient and simple way. PeerJ 6:e4958. PeerJ Inc.

Campitelli, E. 2023. ggnewscale: Multiple Fill and Colour Scales in "ggplot2."

Capella-Gutierrez, S., J. M. Silla-Martinez, and T. Gabaldon. 2009. trimAl: a tool for automated alignment trimming in large-scale phylogenetic analyses. Bioinformatics 25:1972–1973.

Castellanos, M. C., P. Wilson, and J. D. Thomson. 2004. 'Anti-bee' and 'pro-bird' changes during the evolution of hummingbird pollination in *Penstemon* flowers. J. Evol. Biol. 17:876–885.

Chen, L., A. L. DeVries, and C.-H. C. Cheng. 1997. Convergent evolution of antifreeze glycoproteins in Antarctic notothenioid fish and Arctic cod. Proc. Natl. Acad. Sci. 94:3817–3822. Proceedings of the National Academy of Sciences.

Cheng, H., G. T. Concepcion, X. Feng, H. Zhang, and H. Li. 2021. Haplotype-resolved de novo assembly using phased assembly graphs with hifiasm. Nat. Methods 18:170–175. Nature Publishing Group.

Dellinger, A. S., O. Paun, J. Baar, E. M. Temsch, D. Fernández-Fernández, and J. Schönenberger. 2022. Population structure in Neotropical plants: Integrating pollination biology, topography and climatic niches. Mol. Ecol. 31:2264–2280.

Dobin, A., C. A. Davis, F. Schlesinger, J. Drenkow, C. Zaleski, S. Jha, P. Batut, M. Chaisson, and T. R. Gingeras. 2013. STAR: ultrafast universal RNA-seq aligner. Bioinformatics 29:15–21.

Driver, R. 2022. Evolution of olfactory receptors in birds. East Carolina University.

Driver, R. J., and C. N. Balakrishnan. 2021. Highly Contiguous Genomes Improve the Understanding of Avian Olfactory Receptor Repertoires. Integr. Comp. Biol. 61:1281–1290.

Eddy, S. R. 2011. Accelerated Profile HMM Searches. PLOS Comput. Biol. 7:e1002195.

Farré-Armengol, G., I. Filella, J. Llusià, and J. Peñuelas. 2017. β-Ocimene, a Key Floral and Foliar Volatile Involved in Multiple Interactions between Plants and Other Organisms. Molecules 22:1148.

Fu, L., B. Niu, Z. Zhu, S. Wu, and W. Li. 2012. CD-HIT: accelerated for clustering the next-generation sequencing data. Bioinformatics 28:3150–3152.

Gamba, D., and N. Muchhala. 2023. Pollinator type strongly impacts gene flow within and among plant populations for six Neotropical species. Ecology 104:e3845.

Gershenzon, J., and N. Dudareva. 2007. The function of terpene natural products in the natural world. Nat. Chem. Biol. 3:408–414.

Goldsmith, K. M., and T. H. Goldsmith. 1982. Sense of Smell in the Black-Chinned Hummingbird. The Condor 84:237.

Götz, S., J. M. García-Gómez, J. Terol, T. D. Williams, S. H. Nagaraj, M. J. Nueda, M. Robles, M. Talón, J. Dopazo, and A. Conesa. 2008. High-throughput functional annotation and data mining with the Blast2GO suite. Nucleic Acids Res. 36:3420–3435.

Grabherr, M. G., B. J. Haas, M. Yassour, J. Z. Levin, D. A. Thompson, I. Amit, X. Adiconis, L. Fan, R. Raychowdhury, Q. Zeng, Z. Chen, E. Mauceli, N. Hacohen, A. Gnirke, N. Rhind, F. di Palma, B. W. Birren, C. Nusbaum, K. Lindblad-Toh, N. Friedman, and A. Regev. 2011. Full-length transcriptome assembly from RNA-Seq data without a reference genome. Nat. Biotechnol. 29:644–652. Nature Publishing Group.

Graham, A. M., J. M. Jamison, M. Bustos, C. Cournoyer, A. Michaels, J. S. Presnell, R. Richter, D. E. Crocker, A. Fustukjian, M. E. Hunter, L. D. Rea, J. Marsillach, C. E. Furlong, W. K. Meyer, and N. L. Clark. 2023. Reduction of Paraoxonase Expression Followed by Inactivation across Independent Semiaquatic Mammals Suggests Stepwise Path to Pseudogenization. Mol. Biol. Evol. 40:msad104.

Gwinner, H., and S. Berger. 2008. Starling males select green nest material by olfaction using experience-independent and experience-dependent cues. Anim. Behav. 75:971–976.

Haas, B. J., A. Papanicolaou, M. Yassour, M. Grabherr, P. D. Blood, J. Bowden, M. B. Couger, D. Eccles, B. Li, M. Lieber, M. D. MacManes, M. Ott, J. Orvis, N. Pochet, F. Strozzi, N. Weeks, R. Westerman, T. William, C. N. Dewey, R. Henschel, R. D. LeDuc, N. Friedman, and A. Regev. 2013. De novo transcript sequence reconstruction from RNA-seq using the Trinity platform for reference generation and analysis. Nat. Protoc. 8:1494–1512. Nature Publishing Group.

Hagelin, J. C. 2007. The citrus-like scent of crested auklets: reviewing the evidence for an avian olfactory ornament. J. Ornithol. 148:195–201.

Harenčár, J., O. M. Vargas, M. Escalona, D. W. Schemske, and K. M. Kay. 2023. Genome assemblies and comparison of two neotropical spiral gingers: *Costus pulverulentus* and *C. lasius*. J. Hered. esad018.

Hervé, M. 2021. RVAideMemoire: Testing and Plotting Procedures for Biostatistics. R package version 0.9-81.

Hoang, D. T., O. Chernomor, A. von Haeseler, B. Q. Minh, and L. S. Vinh. 2018. UFBoot2: Improving the Ultrafast Bootstrap Approximation. Mol. Biol. Evol. 35:518–522. Oxford Academic.

Janzen, D. H. 1981. Bee Arrival at Two Costa Rican Female Catasetum Orchid Inflorescences, and a Hypothesis on Euglossine Population Structure. Oikos 36:177–183.

Janzen, D. H. 1971. Euglossine Bees as Long-Distance Pollinators of Tropical Plants. Science 171:203–205.

Kalyaanamoorthy, S., B. Q. Minh, T. K. F. Wong, A. von Haeseler, and L. S. Jermiin. 2017. ModelFinder: fast model selection for accurate phylogenetic estimates. Nat. Methods 14:587–589.

Katoh, K., and D. M. Standley. 2013. MAFFT Multiple Sequence Alignment Software Version 7: Improvements in Performance and Usability. Mol. Biol. Evol. 30:772–780. Oxford Academic.

Kay, K. M., and D. L. Grossenbacher. 2022. Evolutionary convergence on hummingbird pollination in Neotropical *Costus* provides insight into the causes of pollinator shifts. New Phytol. 236:1572–1583.

Kay, K. M., and D. W. Schemske. 2003. Pollinator Assemblages and Visitation Rates for 11 Species of Neotropical *Costus* (Costaceae). Biotropica 35:198–207.

Knudsen, J. T., L. Tollsten, I. Groth, G. Bergstöm, and R. A. Raguso. 2004. Trends in floral scent chemistry in pollination syndromes: floral scent composition in hummingbird-pollinated taxa. Bot. J. Linn. Soc. 146:191–199.

Krauss, S. L., R. D. Phillips, J. D. Karron, S. D. Johnson, D. G. Roberts, and S. D. Hopper. 2017. Novel Consequences of Bird Pollination for Plant Mating. Trends Plant Sci. 22:395–410.

Langmead, B., and S. L. Salzberg. 2012. Fast gapped-read alignment with Bowtie 2. Nat. Methods 9:357–359. Nature Publishing Group.

Lanier, E. R., T. B. Andersen, and B. Hamberger. 2023. Plant terpene specialized metabolism: complex networks or simple linear pathways? Plant J. 114:1178–1201.

Li, H. 2018. Minimap2: pairwise alignment for nucleotide sequences. Bioinformatics 34:3094–3100.

Liao, Y., G. K. Smyth, and W. Shi. 2014. featureCounts: an efficient general purpose program for assigning sequence reads to genomic features. Bioinforma. Oxf. Engl. 30:923–930.

Liu, J. W., P. Milet-Pinheiro, G. Gerlach, M. Ayasse, C. E. P. Nunes, I. Alves-Dos-Santos, and S. R. Ramírez. 2024. Macroevolution of floral scent chemistry across radiations of male euglossine bee-pollinated plants. Evolution 78:98–110.

Losos, J. B. 2011. CONVERGENCE, ADAPTATION, AND CONSTRAINT. Evolution 65:1827–1840.

Maas, P. J. M. 1972. Costoideae (Zingiberaceae). Flora Neotropica 8:1–139. New York Botanical Garden Press.

Maas, P. J. M. 1977. Renealmia (Zingiberaceae - Zingiberoideae) Costoideae (Additions) (Zingiberaceae). Flora Neotropica 18:1–218. New York Botanical Garden Press.

Manni, M., M. R. Berkeley, M. Seppey, F. A. Simão, and E. M. Zdobnov. 2021. BUSCO Update: Novel and Streamlined Workflows along with Broader and Deeper Phylogenetic Coverage for Scoring of Eukaryotic, Prokaryotic, and Viral Genomes. Mol. Biol. Evol. 38:4647–4654.

Martin, M. 2011. Cutadapt removes adapter sequences from high-throughput sequencing reads. EMBnet.journal 17:10–12.

Moran, D., R. Softley, and E. J. Warrant. 2015. The energetic cost of vision and the evolution of eyeless Mexican cavefish. Sci. Adv. 1:e1500363. American Association for the Advancement of Science.

Müller, K., and H. Wickham. 2022. tibble: Simple Data Frames.

Nevitt, G. A., M. Losekoot, and H. Weimerskirch. 2008. Evidence for olfactory search in wandering albatross, *Diomedea exulans*. Proc. Natl. Acad. Sci. 105:4576–4581.

Nguyen, L.-T., H. A. Schmidt, A. von Haeseler, and B. Q. Minh. 2015. IQ-TREE: A Fast and Effective Stochastic Algorithm for Estimating Maximum-Likelihood Phylogenies. Mol. Biol. Evol. 32:268–274.

Oksanen, J., F. Guillaume Blanchet, M. Friendly, R. Kindt, P. Legendre, D. McGlinn, P. Minchin, R. O'Hara, G. Simpson, P. Solymos, H. Stevens, E. Szoecs, and H. Wagner. 2020. vegan: Community Ecology Package. R package version 2.5-7.

Opedal, Ø. H., M. Falahati-Anbaran, E. Albertsen, W. S. Armbruster, R. Pérez-Barrales, H. K. Stenøien, and C. Pélabon. 2017. Euglossine bees mediate only limited long-distance gene flow in a tropical vine. New Phytol. 213:1898–1908.

Orr, H. A. 2005. The Probability of Parallel Evolution. Evolution 59:216–220.

Paradis, E., and K. Schliep. 2018. ape 5.0: an environment for modern phylogenetics and evolutionary analyses in R. Bioinformatics, doi: 10.1093/bioinformatics/bty633.

Pedersen, T. L., and F. Crameri. 2023. scico: Colour Palettes Based on the Scientific Colour-Maps.

Peng, F., K. J. R. P. Byers, and H. D. Bradshaw Jr. 2017. Less is more: Independent loss-of-function OCIMENE SYNTHASE alleles parallel pollination syndrome diversification in monkeyflowers (*Mimulus*). Am. J. Bot. 104:1055–1059.

Petrén, H., T. G. Köllner, and R. R. Junker. 2023. Quantifying chemodiversity considering biochemical and structural properties of compounds with the R package chemodiv. New Phytol. 237:2478–2492.

Pichersky, E., and R. A. Raguso. 2018. Why do plants produce so many terpenoid compounds? New Phytol. 220:692–702.

Powers, J., K. Eisen, D. Campbell, and R. Raguso. 2023. bouquet: Filter and Augment Biological GC-MS Data.

R Core Team. 2023. R: A language and environment for statistical computing. R Foundation for Statistical Computing, Vienna, Austria.

Raguso, R. A. 2016. Plant Evolution: Repeated Loss of Floral Scent — A Path of Least Resistance? Curr. Biol. 26:R1282–R1285.

Ramos, S. E., and F. P. Schiestl. 2019. Rapid plant evolution driven by the interaction of pollination and herbivory. Science 364:193–196. American Association for the Advancement of Science.

Revell, L. J. 2012. phytools: an R package for phylogenetic comparative biology (and other things). Methods Ecol. Evol. 3:217–223.

Robinson, M. D., D. J. McCarthy, and G. K. Smyth. 2010. edgeR: a Bioconductor package for differential expression analysis of digital gene expression data. Bioinformatics 26:139–140.

Robinson, M. D., and A. Oshlack. 2010. A scaling normalization method for differential expression analysis of RNA-seq data. Genome Biol. 11:R25.

Rosas-Guerrero, V., R. Aguilar, S. Martén-Rodríguez, L. Ashworth, M. Lopezaraiza-Mikel, J. M. Bastida, and M. Quesada. 2014. A quantitative review of pollination syndromes: do floral traits predict effective pollinators? Ecol. Lett. 17:388–400.

Sackton, T. B., and N. Clark. 2019. Convergent evolution in the genomics era: new insights and directions. Philos. Trans. R. Soc. B Biol. Sci. 374:20190102. Royal Society.

Sas, C., F. Müller, C. Kappel, T. V. Kent, S. I. Wright, M. Hilker, and M. Lenhard. 2016. Repeated Inactivation of the First Committed Enzyme Underlies the Loss of Benzaldehyde Emission after the Selfing Transition in *Capsella*. Curr. Biol. 26:3313–3319.

Schemske, D. W., and H. D. Bradshaw. 1999. Pollinator preference and the evolution of floral traits in monkeyflowers (*Mimulus*). Proc. Natl. Acad. Sci. 96:11910–11915. Proceedings of the National Academy of Sciences.

Sifuentes-Romero, I., A. M. Aviles, J. L. Carter, A. Chan-Pong, A. Clarke, P. Crotty, D. Engstrom, P. Meka, A. Perez, R. Perez, C. Phelan, T. Sharrard, M. I. Smirnova, A. J. Wade, and J. E. Kowalko. 2023. Trait Loss in Evolution: What Cavefish Have Taught Us about Mechanisms Underlying Eye Regression. Integr. Comp. Biol. 63:393–406.

Simão, F. A., R. M. Waterhouse, P. Ioannidis, E. V. Kriventseva, and E. M. Zdobnov. 2015. BUSCO: assessing genome assembly and annotation completeness with single-copy orthologs. Bioinformatics 31:3210–3212.

Slater, G. S. C., and E. Birney. 2005. Automated generation of heuristics for biological sequence comparison. BMC Bioinformatics 6:31.

Smid, M., R. R. J. Coebergh van den Braak, H. J. G. van de Werken, J. van Riet, A. van Galen, V. de Weerd, M. van der Vlugt-Daane, S. I. Bril, Z. S. Lalmahomed, W. P. Kloosterman, S. M. Wilting, J. A. Foekens, J. N. M. IJzermans, P. P. L. O. Coene, J. W. T. Dekker, D. D. E. Zimmerman, G. W. M. Tetteroo, W. J. Vles, W. W. Vrijland, R. Torenbeek, M. Kliffen, J. H. Carel Meijer, A. A. vd Wurff, J. W. M. Martens, A. M. Sieuwerts, and on behalf of the MATCH study group. 2018. Gene length corrected trimmed mean of M-values (GeTMM) processing of RNA-seq data performs similarly in intersample analyses while improving intrasample comparisons. BMC Bioinformatics 19:236.

Tarazona, S., P. Furió-Tarí, D. Turrà, A. D. Pietro, M. J. Nueda, A. Ferrer, and A. Conesa. 2015. Data quality aware analysis of differential expression in RNA-seq with NOISeq R/Bioc package. Nucleic Acids Res. 43:e140.

Tarazona, S., F. García-Alcalde, J. Dopazo, A. Ferrer, and A. Conesa. 2011. Differential expression in RNA-seq: a matter of depth. Genome Res. 21:2213–2223.

Tholl, D. 2006. Terpene synthases and the regulation, diversity and biological roles of terpene metabolism. Curr. Opin. Plant Biol. 9:297–304.

Thomson, J. D., and P. Wilson. 2008. Explaining Evolutionary Shifts between Bee and Hummingbird Pollination: Convergence, Divergence, and Directionality. Int. J. Plant Sci. 169:23–38. The University of Chicago Press.

Tsuchimatsu, T., and S. Fujii. 2022. The selfing syndrome and beyond: diverse evolutionary consequences of mating system transitions in plants. Philos. Trans. R. Soc. B Biol. Sci. 377:20200510.

Valderrama, E., J. B. Landis, D. Skinner, P. J. M. Maas, H. Maas-van de Kramer, T. André, N. Grunder, C. Sass, M. Pinilla-Vargas, C. J. Guan, H. R. Phillips, A. M. R. de Almeida, and C. D. Specht. 2022. The genetic mechanisms underlying the convergent evolution of pollination syndromes in the Neotropical radiation of *Costus* L. Front. Plant Sci. 13:874322.

Vargas, O. M., B. Goldston, D. L. Grossenbacher, and K. M. Kay. 2020. Patterns of speciation are similar across mountainous and lowland regions for a Neotropical plant radiation (Costaceae: *Costus*). Evolution 74:2644–2661.

Wessinger, C. A. 2024. How the switch to hummingbird pollination has greatly contributed to our understanding of evolutionary processes. New Phytol. 241:59–64.

Wickham, H. 2009. ggplot2: Elegant Graphics for Data Analysis. Springer-Verlag New York.

Wickham, H. 2007. Reshaping Data with the reshape Package. J. Stat. Softw. 21:1–20.

Wickham, H., R. François, L. Henry, and K. Müller. 2021. dplyr: A Grammar of Data Manipulation. R package version 1.0.7.

Wickham, H., J. Hester, and J. Bryan. 2023. readr: Read Rectangular Text Data.

Wilke, C. O. 2020. cowplot: Streamlined Plot Theme and Plot Annotations for “ggplot2.”

Workman, R., R. Fedak, D. Kilburn, S. Hao, K. Liu, and W. Timp. 2019. High Molecular Weight DNA Extraction from Recalcitrant Plant Species for Third Generation Sequencing.

Wozniak, N., K. Sartori, C. Kappel, L. Zhao, A. Erban, I. Fehrle, F. Jantzen, M. Orsucci, S. Rosa, M. Lenhard, J. Kopka, and A. Sicard. 2022. Convergence and molecular evolution of floral fragrance after independent transitions to self–fertilization. bioRxiv.

Xie, Y. 2023. knitr: A General-Purpose Package for Dynamic Report Generation in R.

Xu, S. 2022. ggstar: Multiple Geometric Shape Point Layer for "ggplot2."

Xu, S., Z. Dai, P. Guo, X. Fu, S. Liu, L. Zhou, W. Tang, T. Feng, M. Chen, L. Zhan, T. Wu, E. Hu, Y. Jiang, X. Bo, and G. Yu. 2021. ggtreeExtra: Compact Visualization of Richly Annotated Phylogenetic Data. Mol. Biol. Evol. 38:4039–4042.

Yost, J. M., and K. M. Kay. 2009. The evolution of postpollination reproductive isolation in *Costus*. Sex. Plant Reprod. 22:247–255.

Yu, G. 2022. Data Integration, Manipulation and Visualization of Phylogenetic Trees. Chapman & Hall.

Yu, G., D. K. Smith, H. Zhu, Y. Guan, and T. T.-Y. Lam. 2017. ggtree: an r package for visualization and annotation of phylogenetic trees with their covariates and other associated data. Methods Ecol. Evol. 8:28–36.

Zdobnov, E. M., D. Kuznetsov, F. Tegenfeldt, M. Manni, M. Berkeley, and E. V. Kriventseva. 2021. OrthoDB in 2020: evolutionary and functional annotations of orthologs. Nucleic Acids Res. 49:D389–D393.

Zu, P., F. P. Schiestl, D. Gervasi, X. Li, D. Runcie, and F. Guillaume. 2020. Floral signals evolve in a predictable way under artificial and pollinator selection in *Brassica rapa*. BMC Evol. Biol. 20:127.

Zytnicki, M. 2017. mmquant: how to count multi-mapping reads? BMC Bioinformatics 18:411.